





Application of Graphene Oxide Nanoparticles to Cementitious Composites to Mitigate the Effects of Attacks by Aggressive Agents

Aplicación de nanopartículas de óxido de grafeno en compuestos cementosos para mitigar los efectos del ataque de agentes agresivos

S. Castro-Lopes ¹, Barbara Simões ², Sergio Peres ³, V. D. Rodrigues ⁴, T. F. A. Santos ⁵, and Romildo Berenguer ⁶

ABSTRACT

This study investigates the potential of adding 0.03% graphene oxide (GO) nanoparticles into cementitious composites, assessing their mechanical performance and resistance to carbonation. The results indicate a 26% increase in compressive strength, from 23.92 to 32.42 MPa, with tensile strength increasing by an average of 1.14 MPa. Furthermore, the composite exhibits 14% lower capillary water absorption, enhancing resistance to moisture ingress. In terms of carbonation resistance, the addition of GO reduces the carbonation front by approximately 46% compared to the reference samples. Service life estimations suggest that, under equivalent exposure conditions, a structure incorporating GO would experience a degradation equivalent to five years, whereas a conventional structure would degrade over 20 years. These findings highlight the effectiveness of GO nanoparticles in enhancing both the mechanical properties and durability of cementitious materials.

Keywords: nanotechnology, performance, mechanical properties, additions, graphene oxide

RESUMEN

Este estudio investiga el potencial de incluir una concentración de 0.03 % de nanopartículas de óxido de grafeno (GO) en compuestos cementosos, evaluando su rendimiento mecánico y resistencia a la carbonatación. Los resultados indican un aumento del 26 % en la resistencia a la compresión, pasando de 23.92 a 32.42 MPa, con un aumento promedio de 1.14 MPa en la resistencia a la tracción. Además, el compuesto mostró una absorción de agua capilar un 14 % menor, mejorando la resistencia a la penetración de humedad. En términos de resistencia a la carbonatación, la adición de GO redujo el frente de carbonatación en aproximadamente un 46 % en comparación con las muestras de referencia. Las estimaciones de vida útil sugieren que, bajo condiciones de exposición equivalentes, una estructura que incorpore GO experimentaría una degradación equivalente a cinco años, mientras que una estructura convencional se degradaría en más de 20 años. Estos resultados destacan la efectividad de las nanopartículas de GO para mejorar tanto las propiedades mecánicas como la durabilidad de los materiales cementosos.

Palabras clave: nanotecnología, desempeño, propiedades mecánicas, adiciones, óxido de grafeno

Received: November 17th, 2024

Accepted: March 6th, 2025

Introduction

The field of civil construction is one of the most dynamic sectors in Brazil's economy, playing a fundamental role in providing services and materials for the industry [1]. However, despite its positive contributions, this sector also has a significant environmental impact. [2] state that the construction industry consumes over 30% of the natural resources, and that 75% of the waste it generates is neither recycled nor reused. In light of these challenges, there has been increasing interest from both the industry and government entities in developing construction materials with higher durability and better performance to minimize their environmental footprint [3]–[5]. Among the strategies for sustainable development, recent studies have investigated alternative binders, e.g., partially replacing cement with gypsum [6], as well as supplementary cementitious materials like slag cement and rice husk ash to reduce the demand

¹ Civil engineer, Santo Agostinho University Center, UNIFSA, Brazil. PhD in Materials Science, Universidade Federal de Pernambuco, Recife (PE), Brazil. Affiliation: Full professor, Instituto Federal do Pará, IFPA, Brazil. Email: samuel.jonatas@ufpe.br

² Civil engineer, Universidade de Pernambuco, Escola Politécnica de Pernambuco, Recife (PE), Brazil. Affiliation: Young researcher, Universidade de Pernambuco, Brazil. E-mail: bls1@poli.br

³ Mechanical engineer, Universidade Federal de Pernambuco, Recife (PE), Brazil. PhD in Mechanical Engineering, University of Florida, United States of America. Affiliation: Associate professor, Universidade de Pernambuco, Brazil. Email: speres@poli.br

⁴ Biotecnologia, Universidade Presidente Antônio Carlos, Brazil. PhD in Genetics and Molecular Biology, Universidade Estadual de Campinas, Brazil. Affiliation: Researcher, Universidade Federal de Pernambuco, Recife (PE), Brazil. Email: vivibiotec@gmail.com / viviane.drumonnd@ufpe.br

⁵ Graduate in Physics, Universidade Federal de Ouro Preto, UFOP, Brazil. PhD in Mechanical Engineering, Universidade Estadual de Campinas, Brazil. Affiliation: Full professor, Universidade Federal de Pernambuco, Recife (PE), Brazil. Email: tiago.felipe@ufpe.br

⁶ Civil engineer, Universidade Federal de Pernambuco, Recife (PE), Brazil. PhD in Materials Science, Universidade Federal de Pernambuco, Recife (PE), Brazil. Affiliation: Full professor, Universidade de Pernambuco, Escola Politécnica de Pernambuco, Recife (PE), Brazil. Email: romildo.berenguer@upe.br



Attribution 4.0 International (CC BY 4.0) Share - Adapt

for Portland cement [7]. Additionally, the incorporation of recycled concrete aggregate (RCA) in precast concrete has been highlighted as a potential approach to enhancing sustainability in the construction sector [8].

Nanotechnology, introduced as a scientific concept by Norio Taniguchi in 1974, has brought significant advancements across multiple fields, including civil engineering [9]. A simplified definition of nanotechnology involves the exploration of systems at the nanoscale, down to atomic precision, enabling the creation of materials with tailored structures that exhibit unique properties [10]. Over time, the integration of nanotechnology in civil engineering has proven beneficial for enhancing material performance, particularly in improving mechanical strength and durability while reducing the exploitation of natural resources [11]. Among the innovative materials being explored, shape memory alloy fibers such as Ni-Ti have demonstrated the ability to enhance crack recovery in engineered cementitious composites, improving mechanical performance and extending service life [12]. Furthermore, the optimization of cementitious systems with alumina-rich materials has been investigated to improve workability, hydration kinetics, and early-age mechanical performance [13]. Concrete durability is a crucial factor in ensuring that structures perform as intended throughout their service life. The reduction in durability can be attributed to both external environmental factors and intrinsic material deficiencies [14]. Additionally, permeability plays a critical role in determining the extent to which fluids and gases can penetrate concrete, leading to material degradation over time [15].

In response to these challenges, research has focused on applying nanomaterials to concrete and mortar in order to enhance their durability, with carbon-based nanomaterials emerging as promising additives [16]. Among these, graphene oxide (GO) has gained considerable attention in civil engineering, given its high specific surface area, excellent dispersion in water [17], [18], and superior mechanical properties, including its high tensile strength and elastic modulus [19]. Some studies have also indicated that GO may improve the resistance of cementitious materials to aggressive agents, although further research is needed to fully understand these effects.

In this vein, this study investigates the effects of GO nanoparticles on cementitious composites. To this effect, the synthesis of GO nanoparticles is detailed in the supplementary material. Therefore, the research focuses on three main objectives: (i) to assess GO's enhancement of tensile and compressive strength; (ii) to evaluate its reduction in capillary absorption; and (iii) to examine the improved resistance to carbonation attack that it provides. Based on the existing literature, it is hypothesized that the incorporation of GO leads to improved mechanical properties and increased durability of cementitious composites, making them more resistant to environmental factors such as moisture ingress and carbonation.

The document is organized as follows. The next section outlines the materials and methods used to prepare the cementitious composites and conducting the experiments. Subsequently, the results of the mechanical tests, permeability assessments, and carbonation resistance studies are presented, and the final section discusses the conclusions of this study, which demonstrate the significant improvements in the mechanical performance and durability of cementitious composites through the incorporation of GO nanoparticles at a 0.03% concentration.

Materials and methods

This section characterizes the fine aggregate (sand) and Portland CPV-ARI cement used in this research. The fine aggregate was characterized according to [20]. For the chemical and physical characterization of the cement, a literature review was conducted to obtain the necessary data. The physical characterization tests for CPV-ARI cement included unit mass, specific gravity, specific surface area (Blaine), particle size distribution, and loss on ignition. To quantitatively analyze the cement's chemical composition, X-ray fluorescence spectroscopy (FRX) was employed. The physical characterization tests were conducted following established standards, and the results are presented in Tables I and II. The loss on ignition value, expressed as a mass percentage, complies with the provisions of [21], as it remains below the 6.5% limit [22].

Table I. Physical characterization, particle distribution, and loss on ignition of CPV-ARI cement

| Quantity | CPV-ARI cement |
|---|----------------|
| Unit mass (kg/dm ³) | 1.00 |
| Specific gravity (kg/dm ³) | 3.17 |
| Specific surface area (m ² /g) (electronic Blaine) | 0.452 |
| Particle distribution D10 µm | 0.94 |
| Particle distribution D50 µm | 5.9 |
| Particle distribution D90 µm | 29.15 |
| Loss ignition % (LI) | 6.37 |

Source: Authors

Table II. Properties of the reduced graphene oxide (GO) used

| Quantity | Graphene oxide (GO) |
|---|---------------------|
| pH | 2.0-5.0 |
| Tap density (g/cm ³) | <0.1 |
| Specific surface area (m ² /g) | 180-280 |
| H ₂ O | <4.0 |
| Particle size D50 µm | <10.0 |
| C (wt%) | 73 ± 5 |
| O (wt%) | 15 ± 3 |
| S (wt%) | <0.4 |

Source: Authors

Nevertheless, the results presented in Table III confirm that the Portland cement complies with the percentage limits for magnesium oxide ($\text{MgO} \leq 6.5\%$) and sulfur trioxide ($\text{SO}_3 \leq 4.5\%$) established by [21].

Table III. Chemical composition, expressed as a percentage, as obtained via X-ray fluorescence (FRX)

| Quantity | CPV ARI Cement |
|-------------------------|----------------|
| SiO_2 | 19.40 |
| Al_2O_3 | 3.80 |
| CaO | 60.64 |
| Fe_2O_3 | 2.23 |
| TiO_2 | 0.19 |
| MgO | 5.19 |
| K_2O | 0.90 |
| SO_3 | 4.23 |
| Na_2O | 0.45 |
| P_2O_5 | 0.21 |
| MnO | 0.05 |
| Other oxides | 0.03 |

Source: Authors

A sand granulometry analysis was conducted, as it is a crucial indicator of the aggregate's physical and chemical properties, influencing both compaction and resistance to mechanical stresses [20]. The sand used in this study was oven-dried at $105 \pm 5^\circ\text{C}$ and divided into two 500 g samples, as specified in [20]. Two tests (A and B) were performed. A set of standard sieves (4.8, 2.38, 1.19, 0.59, 0.3, and 0.15 mm) was used to carry out the analysis. The sieve set was subjected to agitation for 10 minutes in a mechanical sieving machine, as shown in Fig. S1 (supplementary material), which allowed determining the maximum characteristic dimension and the sand fineness modulus. According to [20], these correspond, respectively, to (i) the particle size at which the accumulated retained percentage of the aggregate is equal to or less than 5%, and (ii) the sum of the accumulated retained percentages in the standard sieves, divided by 100. We observed that the variation limit of $\pm 4\%$ in the retained percentage between tests A and B was respected, as established by [20]. Furthermore, the maximum characteristic dimension (MD) and the sand fineness modulus (FM) were found to be 4.75 and 2.00 mm, respectively. The granulometric composition of the sand used in this research is presented in Fig. S2 (supplementary material) and Table IV.

GO is primarily synthesized through the oxidation of graphite, with the modified Hummers method being the most widely used approach [23], [24]. Initially, the Hummers method employed high proportions of reactive substances. Over time, modifications to this process were introduced, leading to what is now referred to as the *modified Hummers method* [25]. This approach involves the oxidation of graphite using potassium permanganate and sodium nitrate in the presence of concentrated sulfuric acid [23], [26]. According to [27],

[28], this is the most stable and reliable technique for producing two-dimensional GO sheets. It also offers two key advantages: the ability to produce large quantities of GO and the relatively low cost of equipment and reagents [29].

Table IV. Granulometric composition of the sand

| Sieve (mm) | Retained mass (g) Test A | Retained mass (g) Test B | Retained (%) Test A | Retained (%) Test B | Variation ($\pm 4\%$) | Mean (%) | Accumulated (%) |
|------------|--------------------------|--------------------------|---------------------|---------------------|-------------------------|----------|-----------------|
| 4.75 | 3.31 | 2.72 | 0.7 | 0.5 | 0.2 | 0.6 | 0.6 |
| 2.38 | 22.66 | 21.76 | 4.5 | 4.4 | 0.2 | 4.4 | 5.1 |
| 1.19 | 45.09 | 44.04 | 9.0 | 8.8 | 0.2 | 8.9 | 14.0 |
| 0.59 | 97.40 | 94.06 | 19.5 | 18.8 | 0.7 | 19.2 | 33.1 |
| 0.3 | 149.09 | 144.30 | 29.9 | 28.9 | 1.0 | 29.4 | 62.5 |
| 0.15 | 111.80 | 112.54 | 22.4 | 22.5 | 0.1 | 22.5 | 85.0 |
| Pan | 70.07 | 80.04 | 14.0 | 16.0 | 2.0 | 15.0 | 100.0 |
| Total | 499.42 | 499.46 | | | | | |

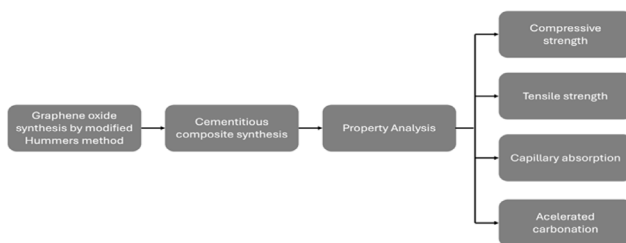
Source: Authors

In this study, GO nanoparticles were synthesized using the modified Hummers method, as illustrated in Figs. S3a to S3f (supplementary material) [30]. The process began with the dispersion of 1 g of graphite in a solution of NaNO_3 and H_2SO_4 , followed by continuous stirring for one hour. Subsequently, 3 g of KMnO_4 were gradually added at a rate of 1 g every 15 minutes while maintaining the solution in an ice bath to prevent the temperature from exceeding 20°C , thereby mitigating the risk of overheating and potential explosions. The mixture was then vigorously stirred before the slow addition of 100 mL of heated distilled water to dilute the solution. Afterwards, 3 mL of a 30% H_2O_2 solution were introduced to ensure the complete reaction of the KMnO_4 , and the mixture was left to settle. Finally, the suspension was washed with HCl and deionized water, followed by filtration and drying to obtain the final GO product [26].

For mortar preparation, 0.1872 g of GO were manually pre-diluted, followed by dispersion using an electromagnetic stirrer for one minute to ensure a uniform distribution before application. The execution of this process, as illustrated in Fig. S4 (supplementary material), follows the procedure described by [28], which has been recognized as an effective method for achieving homogeneous nanoparticle dispersion.

For the preparation of test specimens, samples were produced with and without the addition of GO nanoparticles. These were designated as GO 0.03% and reference samples, respectively, for subsequent analysis and performance comparison. The specimens were molded while following the guidelines of [31], with a mix proportion of 1:3:0.48 (cement:sand:water) by mass. This corresponds to 624 g of cement, 1872 g of sand, and 300 mL of water, resulting in a water-to-cement ratio (w/c) of 0.48. If needed, the water/cement ratio can be determined by measuring the concrete's dielectric constant [32], [33].

The quantity of GO nanoparticles used in each test specimen was 0.03% (0.1872 g) by weight of cement. To facilitate the incorporation of GO into the mortar, a portion of the mix water was removed and used for diluting the GO, which was agitated for a few minutes. The diluted GO was then combined with the remaining water, followed by the addition of cement. The mixing procedures were carried out using a mechanical mortar mixer, as specified in [31]. The mortar was prepared in four layers of approximately equal height, with manual compaction achieved by applying 30 blows per layer using a tamper after applying a release agent to the molds. After molding, the test specimens were left in the molds for 24 hours. A total of 12 cylindrical test specimens were produced, each measuring 5 x 10 cm, six with GO and six without, as shown in Fig. S5 (supplementary material). Flowchart 1 shows the steps of this research.



Flowchart 1. Research stages and development

Source: Authors

Compressive test

After a wet curing period of 28 days, six cylindrical test specimens (three with the addition of GO nanoparticles and three without) were subjected to an axial compression test according to [34]. Before testing, the top surface of the specimens was smoothed using a machine called a *rectifier*. The purpose of the rectifier is to create a smooth and even surface, ensuring that the load applied by the testing machine is distributed uniformly across the material.

Capillary water absorption test

The capillary water absorption test was conducted in accordance with the procedures established by [35]. Water absorption tests were performed on samples both with and without GO in their matrix to analyze potential differences in water absorption capacity between the groups. After 28 days of wet curing, the masses of the test specimens were measured, and they were then placed in an oven at a temperature of 105 ± 5 °C until a constant mass was achieved. Once the steady state had been reached, the dry mass (m_d) of each specimen was determined.

In the second step, the test specimens were positioned on a support and submerged in a container of water, with the water level maintained at 5 ± 1 mm above their lower face. The saturated mass (m_s) of each specimen was recorded at specific time intervals following initial water contact (3, 6, 14, 48, and 72 h).

Tensile strength and accelerated carbonation resistance tests

Tensile strength tests were conducted using the Brazilian method, adhering to all the conditions outlined in [36]. During the diametral compression test for tensile strength, the load required to induce failure in the test specimen was evaluated based on the force applied in the direction of the diameter.

For the accelerated carbonation resistance test, six test specimens without additions (reference samples) and six specimens with GO were prepared. The samples were placed in an oven until a constant mass was achieved and then transferred to a carbonation chamber. The chamber used in this research was a CARON refrigerated CO₂ incubator featuring digital automatic temperature control within ± 1 °C, relative humidity control within $\pm 2\%$, and regulated CO₂ levels.

At predetermined analysis intervals, 30 days after the specimens were placed in the carbonation chamber, each specimen was fractured into three parts. At each evaluation, the carbonation front was verified in slices measuring approximately 3.3 cm of the test specimen. An EMIC press with a maximum capacity of 100 kN was used for specimen rupture, as shown in Fig. 1.



a



b

Figure 1. a) Carbonation tests with reference samples and samples with GO in the first 30 days, b) carbonation test specimens after 90 days
Source: Authors

Results and discussion

Axial compressive strength

For the compressive strength test, 12 specimens were analyzed, six with GO nanoparticles and six without, serving as reference specimens. All specimens were tested after 28 days. The average compressive strength results are presented in Fig. 2.

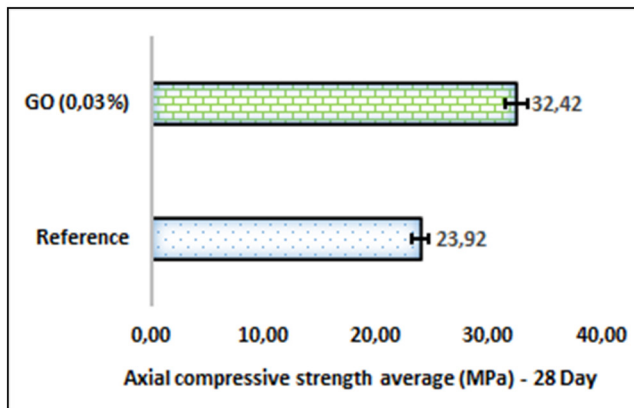


Figure 2. Average compressive strength of both mortar types after 28 days

Source: Authors

An increase in compressive strength was observed in the mortar with the addition of GO in its matrix. The average strength, when compared to the reference mortar, showed an increase of approximately 26%, rising from 23.92 to 32.42 MPa. These results corroborate previous research works that also demonstrated improvements in compressive strength with the addition of 0.03% GO in the mortar. This can be attributed to the excellent dispersion of GO in the cement matrix, the formation of covalent bonds between GO and the cement hydration products, the degree of hydration, and the effect of GO sheets filling the pores of the mortar [37]–[39].

Similarly, machine learning-based approaches have been employed to predict the compressive strength of concrete incorporating alternative materials. [40] proposed a data-driven hybrid machine learning framework to estimate the compressive strength of concrete with rice husk ash (RHA), contributing to mitigating the environmental impact of the cement industry. Additionally, experimental studies reinforce the effectiveness of material modifications in enhancing mechanical properties. [41] demonstrated that adding low concentrations of steel fiber to recycled aggregate concrete can improve its shear strength by more than 51%.

Capillary water absorption

The water absorption capacity of a material is one of the most important transport mechanisms that can affect the

durability of cementitious composites [42]. Fig. 3 presents the comparative results regarding the average water absorption by capillary, expressed as a percentage, for the reference mortar vs. the one with GO addition in each weighing time established by the standard.

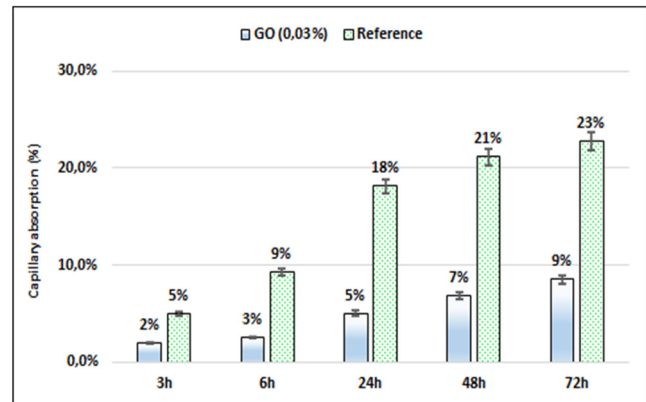
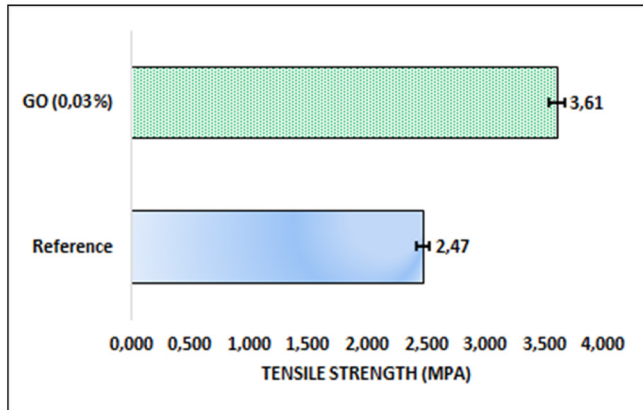


Figure 3. Comparison of results regarding the average water absorption by capillary

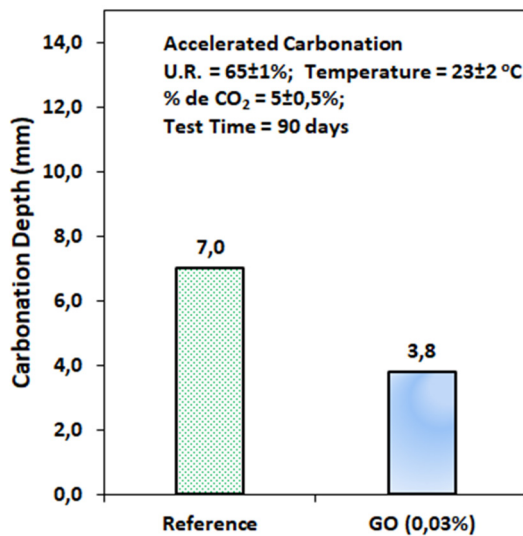
Source: Authors

Fig. 3 shows that the test specimens with the addition of GO exhibited superior performance, characterized by lower capillary absorption compared to the reference samples. In all measurements, the reference samples absorbed more water than those with GO. When analyzing the average absorption for both mortar types, it became evident that, at the final measurement time, the reference samples had a final absorption rate 14% higher than that of the samples containing GO. This behavior may be related to the hydrophobicity of GO, which stems from the presence of oxygenated functional groups on its surface [43]. The hydrophobicity of GO can ensure lower water absorption in samples with nanoparticles, which occasionally ensures superior performance during capillary absorption testing. The easy dispersion of GO in water, due to its oxygenated functional groups, facilitates its incorporation into the cement matrix [16]. Despite this, nanoparticle agglomeration remains a challenge, as van der Waals forces can lead to clustering [44]. However, in this study, it was observed that GO, due to its hydrophobicity, was able to reduce water absorption. [45] demonstrated that the incorporation of colloidal nanosilica (CNS) into concrete can reduce its water absorption. This effect is attributed to enhanced pore filling and the pozzolanic reaction facilitated by nanosilica. Furthermore, the presence of CNS improved cement hydration and produced a greater quantity of CSH gel, thereby enhancing the mechanical properties of the concrete.

Tensile strength and accelerated carbonation resistance



a



b

Figure 4. a) Average tensile strength of both mortar types, b) accelerated carbonation (90 days)

Source: Authors

Fig. 4a illustrates the tensile strength performance of both the reference mortar and the GO-enhanced sample. The reference mortar exhibited a tensile strength of approximately 2.47 MPa, whereas the GO-modified sample reached 3.61 MPa, representing a 46% increase (1.14 MPa). This enhancement can be attributed to improvements in the microstructure of the cementitious matrix; GO facilitates stronger bonding between cement hydration products, resulting in a denser structure with fewer internal defects. Additionally, GO layers act as bridging agents, effectively distributing the applied stresses. Similar findings have been reported for mortars incorporating GO [18], [26], [37]–[39]. [46] demonstrated that integrating hybrid fibers into self-compacting concrete enhances mechanical properties and durability after exposure to high temperatures and freeze-thaw cycles by mitigating crack formation and propagation. Conversely, the incorporation of expanded polystyrene (EPS) spheres reduces the

mechanical strength of concrete – the low density of EPS leads to an overall decline in mechanical performance [47]. In another study, [48] demonstrated that incorporating EPS spheres, silica fume, and superplasticizer into concrete can effectively reduce its weight while significantly enhancing the shear capacity of two-way slabs. [49] proposed a novel cement-based anchoring material and demonstrated that an optimal combination of fly ash (15%), blowing agent (3%), water-reducing agent (0.2%), accelerator (1%), and Huaqiansu (1%) enhances bond strength and improves tensile strength.

Fig. 4b presents the results of the carbonation resistance test. The addition of GO reduced the carbonation front by approximately 46% compared to the reference samples, providing a basis for further analysis regarding service life calculations. These findings suggest that the addition of GO nanoparticles improves the durability of the structure by mitigating carbonation.

The addition of minerals generally improves concrete properties, including durability. However, carbonation can have a negative impact, leading to unfavorable outcomes [50]. Research has shown that the use of fly ash, a medium reactivity pozzolan, significantly increases the rate of carbonation front progression [50]–[53].

On the other hand, the incorporation of supplementary pozzolans like active silica, metakaolin, and rice husk ash, as well as unconventional by-products such as submerged arc welding (SAW) slag, has been shown to improve resistance to carbonation, helping to slow down its advancement [54]–[56]. These pozzolanic reactions refine the pore structure and reduce CO₂ permeability, a result consistent with the findings of [22], [57], [58].

Through Eq. (1), it is possible to evaluate the concrete structure's time of degradation for the two types analyzed, which would correspond to the carbonation front shown in Fig. 4b [58].

$$x = k\sqrt{t} \quad (1)$$

In the equation, x represents the depth of the carbonation front, k is the constant ranging from 0.1 to 1.0 cm²/year, and t denotes the degradation time in years. In this research, with a constant of 0.5 cm²/year, we found that, regarding the reference samples, the structure would experience a degradation equivalent to that of a two-year-old structure. In contrast, the structure with 0.03% GO would only degrade as if it were six months old under the same conditions. Thus, considering a degradation lifespan of 20 years for the reference samples, structures containing GO nanoparticles (0.03%) would only experience a degradation equivalent to five years.

The results suggest that the addition of GO nanoparticles can extend the service life and durability of structures by approximately four times compared to conventional

structures. This indicates a potential for more sustainable construction practices and environmentally friendly building solutions.

[59] conducted a study simulating the incorporation of cellulose nanofibers from agricultural waste as a sustainable cement replacement for producing high-performance concrete. The results indicate that high-performance concrete enhanced with cellulose nanofibers has superior mechanical properties in comparison with conventional high-performance concrete, including improved stress, strain, and equivalent deformation under load. In addition, [60] developed a silica-based superhydrophobic coating to enhance the durability and safety of cementitious surfaces in road construction.

Conclusions

This study demonstrates the significant improvements in both mechanical performance and durability of cementitious composites through the incorporation of graphene oxide nanoparticles at a 0.03% concentration. The results indicate a 26% increase in compressive strength, accompanied by enhanced tensile strength and a reduction in water absorption. Moreover, the inclusion of GO notably improved the resistance to carbonation, with a reduction of approximately 46% in carbonation front progression compared to the reference samples. These findings underscore the potential of GO to enhance the mechanical properties and long-term durability of concrete, offering promising implications for its use in construction materials exposed to aggressive environmental conditions.

Acknowledgements

The authors are grateful for the financial support of the Brazilian Agencies FACEPE, CAPES, and National Council for Scientific and Technological Development (CNPq). The authors also thank Universidade de Pernambuco (POLI/UPE, Brazil), Universidade Federal da Paraíba (UFPB, Brazil), and Universidade Federal de Pernambuco (UFPE, Brazil) for making the equipment available.

CRedit author statement

BS and SCL were in charge of conceptualization, and SP collected the data, developed the workflow, and performed assessments. VDR and TFSA provided critical feedback, led the drafting process, and wrote the main part of the manuscript. RB contributed with supervision and validation, to which all authors contributed.

Conflicts of interest

The authors have no conflicts of interest to declare.

References

- [1] T. A. Frej and L. H. Alencar, "Fatores de sucesso no gerenciamento de múltiplos projetos na construção civil em Recife," *Production*, vol. 20, no. 3, pp. 322-334, Sept. 2010. <https://doi.org/10.1590/S0103-65132010005000043>
- [2] C. K. Purchase *et al.*, "Circular economy of construction and demolition waste: A literature review on lessons, challenges, and benefits," *Materials*, vol. 15, no. 1, art. 76, 2021. <https://doi.org/10.3390/ma15010076>
- [3] A. A. Firoozi, A. A. Firoozi, D. O. Oyejobi, S. Avudaiappan, and E. S. Flores, "Emerging trends in sustainable building materials: Technological innovations, enhanced performance, and future directions," *Results Eng.*, vol. 24, art. 103521, Dec. 2024. <https://doi.org/10.1016/j.rineng.2024.103521>
- [4] N. Makul and G. Suaiam, "New insights into the early age time dependent dielectric evolution of pozzolan modified eco efficient cement pastes within a frequency range of 200 MHz to 6500 MHz: Experiments and statistical modeling," *Eng. Sci.*, vol. 31, art. 1170, 2024. <https://doi.org/10.30919/es1170>
- [5] M. P. Rosa *et al.*, "Viabilidade na reutilização da ardósia em substituição do agregado graúdo na dosagem do concreto," *Braz. J. Dev.*, vol. 6, pp. 936-948, 2020. <https://doi.org/10.34117/bjdv6n1-065>
- [6] N. Gerges *et al.*, "The novelty of partially replacing cement with Gypsum: Optimum mix design and structural applications," *ES Mater. Manuf.*, 2024. [Online]. Available: <https://doi.org/10.30919/esmm1336>
- [7] P. Hiremath *et al.*, "Investigating the mechanical properties, durability, and environmental impact of partial cement substitution with slag cement and rice husk ash for sustainable concrete production," *ES Food Agrofor.*, vol. 18, art. 1267, 2024. <https://doi.org/10.30919/esfaf1267>
- [8] G. Sua-iam and N. Makul, "Potential future direction of the sustainable production of precast concrete with recycled concrete aggregate: A critical review," *Eng. Sci.*, vol. 28, art. 1075, 2024. <https://doi.org/10.30919/es1075>
- [9] N. Taniguchi, "On the basic concept of 'nano-technology'," in *Proc. Intl. Conf. Prod. Eng.*, Tokyo, Japan, 1974, pp. 18-23.
- [10] S.A. Filho and B.P. Backx, "Nanotecnologia e seus impactos na sociedade," *R. Tecnol. Soc.*, vol. 16, no. 40, pp. 1-15, Apr./Jun. 2020. <https://doi.org/10.3895/rt.s.v16n40.9870>
- [11] M. Feizbahr and P. Pourzanjani, "Nanotechnology in construction: Innovations, applications, and impacts authors," *J. Civ. Eng. Res.*, vol. 6, no. 1, pp. 35-4, 2024. <https://doi.org/10.61186/JCER.6.1.35>
- [12] M. Song, J. Wang, L. Yuan, C. Luan, and Z. Zhou, "Investigation on crack recovery behavior of engineered cementitious composite (ECC) incorporated memory alloy fiber at low temperature," *ES Mater. Manuf.*, vol. 17, pp. 23-33, 2022. <https://doi.org/10.30919/esmm5f662>
- [13] S. Al-Sherei, H. A. Abdel-Gawwad, and M. S. Meddah, "Unveiling the influence of varied alumina sources on fresh properties of ordinary Portland cement mortar and concrete: A comprehensive review," *Eng. Sci.*, vol. 30, art. 1118, 2024. <https://doi.org/10.30919/es1118>

- [14] R. M. Ferreira, "Avaliação dos ensaios de durabilidade do betão," Master's thesis, Esc. Eng., Univ. do Minho, Braga, Portugal, 2000.
- [15] L. A. Araujo *et al.*, "Concrete gas permeability: Implications for hydrogen storage applications," *Appl. Sci.*, vol. 14, no. 15, art. 6408, 2024. <https://doi.org/10.3390/app14156408>
- [16] A. Bagheri, E. Negahban, A. Asad, H.A. Abbasi, S.M. Raza, "Graphene oxide-incorporated cementitious composites: a thorough investigation," *Mater. Adv.*, vol. 3, pp. 9040-9051, 2022. <https://doi.org/10.1039/D2MA00169A>
- [17] S. Chuah, Z. Pan, J. G. Sanjayan, C. M. Wang, and W. H. Duan, "Nano reinforced cement and concrete composites and new perspective from graphene oxide," *Constr. Build. Mater.*, vol. 73, pp. 113-124, Dec. 2014. <https://doi.org/10.1016/j.conbuildmat.2014.09.040>
- [18] Y. Y. Wu, L. Que, Z. Cui, and P. Lambert, "Physical properties of concrete containing graphene oxide nanosheets," *Materials*, vol. 12, no. 10, art. 1707, May. 2019. <https://doi.org/10.3390/ma12101707>
- [19] M. Frąc, W. Pichór, and P. Szołdra, "Cement composites with expanded graphite as resistance heating elements," *J. Compos. Mater.*, vol. 54, no. 25, pp. 3821-2831, 2020. <https://doi.org/10.1177/0021998320921510>
- [20] *Aggregates - Sieve analysis of fine and coarse aggregates*, NBR NM 248, Brazilian Association of Technical Standards, Rio de Janeiro, Brazil, 2003.
- [21] *Portland cement - Requirements*, NBR 16697, Brazilian Association of Technical Standards, Rio de Janeiro, Brazil, 2018.
- [22] R. Berenguer, A. P. B. Capraro, M. H. F. Medeiros, A. M. P. Carneiro, R. A. Oliveira, "Sugar cane bagasse ash as a partial substitute of Portland cement: Effect on mechanical properties and emission of carbon dioxide," *J. Environ. Chem. Eng.*, vol. 8, no. 2, art. 103655, Apr. 2020. <https://doi.org/10.1016/j.jece.2020.103655>
- [23] G. Dias, T. Cellet, M. Santos, C. Carvalho, and L. Malmonge, "A caracterização morfológica de óxido de grafeno preparados pelo método de Hummers modificado," *Rev. Tecnol.*, vol. 29, no. 1, pp. 199-216, 2020. <https://doi.org/10.4025/revtecnol.v29i1.51286>
- [24] S. Park and R. S. Ruoff, "Chemical methods for the production of graphenes," *Nature Nanotech.*, vol. 4, pp. 217-224, Apr. 2009. <https://doi.org/10.1038/nnano.2009.58>
- [25] J. E. D. Vieira Segundo and E. O. Vilar, "Grafeno: Uma revisão sobre propriedades, mecanismos de produção e potenciais aplicações em sistemas energéticos," *REMAP*, vol. 11, no. 2, pp. 54-57, 2016. <https://remap.revistas.ufcg.edu.br/index.php/remap/article/viewFile/493/387>
- [26] M. M. Mokhtar, S. A. Abo-El-Enein, M. Y. Hassaan, M. S. Morsy, and M. H. Khalil, "Mechanical performance, pore structure and micro-structural characteristics of graphene oxide nanoplatelets reinforced cement," *Constr. Build. Mater.*, vol. 138, pp. 333-339, May. 2017. <https://doi.org/10.1016/j.conbuildmat.2017.02.021>
- [27] S. Stankovich *et al.*, "Graphene-based composite materials," *Nature*, vol. 442, pp. 282-286, Jul. 2006. <https://doi.org/10.1038/nature04969>
- [28] C. S. R. Indukuri and R. Nerella, "Enhanced transport properties of graphene oxide-based cement composite material," *J. Build. Eng.*, vol. 37, art. 102174, May. 2021. <https://doi.org/10.1016/j.jobbe.2021.102174>
- [29] R. Hack, C. Correia, R. Zanon, and S. Pezzin, "Characterization of graphene nanosheets obtained by a modified Hummer's method," *Matéria (Rio J.)*, vol. 23, no. 1, 2018. <https://doi.org/10.1590/S1517-707620170001.0324>
- [30] A. Alazmi, S. Rasul, S. P. Patole, and P. M. F. J. Costa, "Comparative study of synthesis and reduction methods for graphene oxide," *Polyhedron*, vol. 116, pp. 153-161, Sep. 2016. <https://doi.org/10.1016/j.poly.2016.04.044>
- [31] *Portland cement - Determination of compressive strength of cylindrical test specimens*, NBR 7215, Brazilian Association of Technical Standards, Rio de Janeiro, Brazil, 2019.
- [32] R. He, T. Nantung, J. Olek, and N. Lu, "Use of dielectric constant for determination of water-to-cement ratio (W/C) in plastic concrete: part 2: comparison determined W/C values by ground penetrating radar (GPR) and microwave oven drying measurements," *ES Mater. Manuf.*, vol. 22, art. 874, 2023. <https://doi.org/10.30919/esmm5f874>
- [33] R. He, T. Nantung, and J. Olek, N. Lu, "Use of dielectric constant for determination of water-to-cement ratio (W/C) in plastic concrete: part 1. Volumetric water content modeling," *ES Mater. Manuf.*, vol. 21, art. 866, 2023. <https://doi.org/10.30919/esmm5f866>
- [34] *Concrete - Compression test of cylindrical specimens*, NBR 5739, Brazilian Association of Technical Standards, Rio de Janeiro, Brazil, 2018.
- [35] *Mortar and hardened concrete - Determination of water absorption by capillarity*, NBR 9779, Brazilian Association of Technical Standards, Rio de Janeiro, Brazil, 2012.
- [36] *Concrete and mortar - Determination of the tension strength by diametrical compression of cylindrical test specimens*, NBR 7222, Brazilian Association of Technical Standards, Rio de Janeiro, Brazil, 2011.
- [37] K. Gong *et al.*, "Reinforcing effects of graphene oxide on Portland cement paste," *J. Mater. Civ. Eng.*, vol. 27, no. 2, Jul. 2015. [https://doi.org/10.1061/\(ASCE\)MT.1943-5533.0001125](https://doi.org/10.1061/(ASCE)MT.1943-5533.0001125)
- [38] S. Lv, Y. Ma, C. Qiu, T. Sun, J. Liu, and Q. Zhou, "Effect of graphene oxide nanosheets of microstructure and mechanical properties of cement composites," *Constr. Build. Mater.*, vol. 49, pp. 121-127, Dec. 2013. <https://doi.org/10.1016/j.conbuildmat.2013.08.022>
- [39] Y. Wang, J. Yang, and D. Ouyang, "Effect of graphene oxide on mechanical properties of cement mortar and its strengthening mechanism," *Materials*, vol. 12, no. 22, art. 3753, 2019. <https://doi.org/10.3390/ma1223753>
- [40] R. Odeh, R. Alawadi, A. Tarawneh, A. Alghossoon, R. Al-Mazaidh, and H. Amerah, "Estimating rice husk ash concrete compressive strength using hybrid machine learning methodology," *Eng. Sci.*, vol. 29, art. 1111, 2024. <https://doi.org/10.30919/es1111>
- [41] S. Leelatanon, T. Imjai, M. Setkit, R. Garcia, and C. K. Ma, "Shear strength of stirrup-free recycled aggregate concrete beams reinforced with steel fibers," *Eng. Sci.*, vol. 31, art. 1249, 2024. <https://doi.org/10.30919/es1249>

- [42] G. L. Golewski, "Assessing of water absorption on concrete composites containing fly ash up to 30 % in regards to structures completely immersed in water," *Case Stud. Const. Mater.*, vol. 19, art. e02337, 2023. <https://doi.org/10.1016/j.cscm.2023.e02337>
- [43] L. Qiu *et al.*, "Dispersing carbon nanotubes with graphene oxide in water and synergistic effects between graphene derivatives," *Chem. - Eur. J.*, vol. 16, no. 35, art. 10653-10658, Sep. 2010. <https://doi.org/10.1002/chem.201001771>
- [44] S. Parveen, S. Rana, and R. Figueiro. "A review on nano-material dispersion, microstructure and mechanical properties of carbon nanotube and nanofiber-based cement composites," *J. Nanomater.*, vol. 2013, art. 710175, 2013. <https://doi.org/10.1155/2013/710175>
- [45] C. Huang, Y. F. Su, R. Tokpatayeva, T. Nantung, and N. Lu, "Investigation of internal curing efficacy of Portland cement concrete incorporated with colloidal nano silica," *ES Mater. Manuf.*, vol. 20, art. 798, 2022. <https://doi.org/10.30919/esmm5f798>
- [46] A. Ashteyat, A. Obaidat, and R. Qerba, "The rheological, mechanical, and durability behavior of self-compacted concrete (SCC) mixed with hybrid fibers after exposure to high temperatures and cycles of freezing and thawing," *Eng. Sci.*, vol. 27, art. 1042, 2023. <https://doi.org/10.30919/es1042>
- [47] M. Abdel-Jaber, R. Al-Nsour, N. Shatarat, H. Katkhuda, and H. Al-zu'bi, "Thermal effect on the flexural performance of lightweight reinforced concrete beams using expanded polystyrene beads and pozzolana aggregate," *Eng. Sci.*, vol. 27, art. 1029, 2023. <https://doi.org/10.30919/es1029>
- [48] M. Abdel-Jaber, N. Shatarat, H. Katkhuda, and M. Al-Najjar, "Punching shear capacity of polystyrene lightweight concrete two-way slabs," *Eng. Sci.*, vol. 31, art. 1216, 2024. <https://doi.org/10.30919/es1216>
- [49] S. Huang, X. Meng, G. Zhao, and Z. Liu, "Development and engineering application of cement-based full length anchoring material," *ES Mater. Manuf.*, vol. 23, art. 1051, 2023. <https://doi.org/10.30919/esmm1051>
- [50] J. Khunthongkeaw, S. Tangtermsirikul, and T. Leelawat, "A study on carbonation depth prediction for fly ash concrete," *Constr. Build. Mater.*, vol. 20, no. 9, pp. 744-753, Nov. 2006. <https://doi.org/10.1016/j.conbuildmat.2005.01.052>
- [51] S. Rukzon and P. Chindaprasirt, "Strength and carbonation model of rice husk ash cement mortar with different fineness," *J. Mater. Civ. Eng.*, vol. 22, no. 3, pp. 253-259, Feb. 2010. [https://doi.org/10.1061/\(ASCE\)0899-1561\(2010\)22:3\(253\)](https://doi.org/10.1061/(ASCE)0899-1561(2010)22:3(253))
- [52] É. Sousa, A. Santana, M. Moura, J. M. P. Q. Delgado, and R. Berenguer, "Thermography applied to the adhesion phenomenon of mortars with additions of submerged arc welding (SAW) slag," *Buildings*, vol. 14, no. 9, art. 2960, 2024. <https://doi.org/10.3390/buildings14092960>
- [53] A. Younsi, P. Turcry, A. Ait-Mokhtar, and S. Staquet, "Accelerated carbonation of concrete with high content of mineral additions: Effect of interactions between hydration and drying," *Cem. Concr. Res.*, vol. 43, pp. 25-33, Jan. 2013. <https://doi.org/10.1016/j.cemconres.2012.10.008>
- [54] K. Turk, M. Karatas, and T. Gonen, "Effect of fly ash and silica fume on compressive strength, sorptivity and carbonation of SCC," *KSCE J. Civ. Eng.*, vol. 17, no. 1, pp. 202-209, Jan. 2013. <https://doi.org/10.1007/s12205-013-1680-3>
- [55] M. V. Moura, S. A. Paiva, V. D. Rodrigues, S. J. Lopes, T. F. Santos, and R. A. Berenguer, "Analysis of the influence of mechanical properties of cementitious composites using submerged arc welding (SAW) slag recycled aggregate," *GESEC*, vol. 15, no. 13, art. e3623, 2024. <https://doi.org/10.7769/gesec.v15i3.3623>
- [56] R. A. Berenguer, *et al.*, "Cement-based materials: Pozzolanic activities of mineral additions are compromised by the presence of reactive oxides," *J. Build. Eng.*, vol. 41, art. 102358, Sep. 2021. <https://doi.org/10.1016/j.jobbe.2021.102358>
- [57] R. A. Berenguer *et al.*, "Durability of concrete structures with sugar cane bagasse ash," *Adv. Mater. Sci. Eng.*, vol. 2020, art. 6907834, 2020. <https://doi.org/10.1155/2020/6907834>
- [58] M. H. F. Medeiros, J. J. O. Andrade, and P. Helene, "Durabilidade e vida útil das estruturas de concreto," in *Concreto: Ciência e Tecnologia*, ed. 1. São Paulo, Brazil: IBRA-CON, 2011, ch. 22.
- [59] M. D. Sreeja and N. Nalanth, "Exploring environmentally sustainable concrete: An analytical investigation on high performance concrete using cellulose nanofibers," *ES Ener. Environ.*, vol. 27, art. 1382, 2025. <https://doi.org/10.30919/esee1382>
- [60] N. Kydyrbay *et al.*, "Enhancing road durability and safety: a study on silica-based superhydrophobic coating for cement surfaces in road construction," *Eng. Sci.*, vol. 30, art. 1221, 2024. <https://doi.org/10.30919/es1221>

Supplementary Material

1 Materials and Methods

The sand granulometry analysis was conducted since it is a key indicator of the aggregate's physical and chemical properties, influencing compaction and mechanical resistance. The sand was oven-dried at $105 \pm 5^\circ\text{C}$ and divided into two 500 g samples. Two tests, A and B, were performed using a standard sieve set (4.8, 2.38, 1.19, 0.59, 0.3, and 0.15 mm).

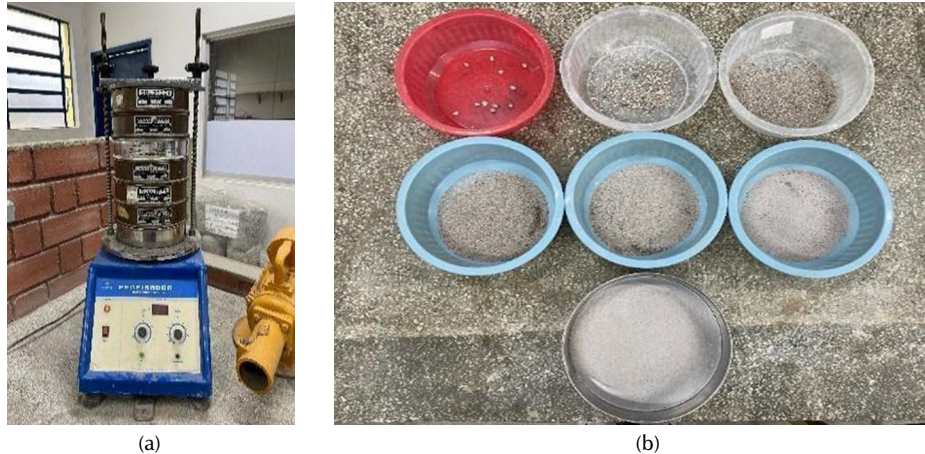


Figure S1 - (a) Mechanical sieve and (b) - Granulometry test
Source: Authors

The sieve set was agitated for 10 minutes using a mechanical sieving machine, as shown in Fig. S1. This process determined the maximum particle size and the sand fineness modulus. The granulometric composition of the sand used in this study is presented in Fig. S2.

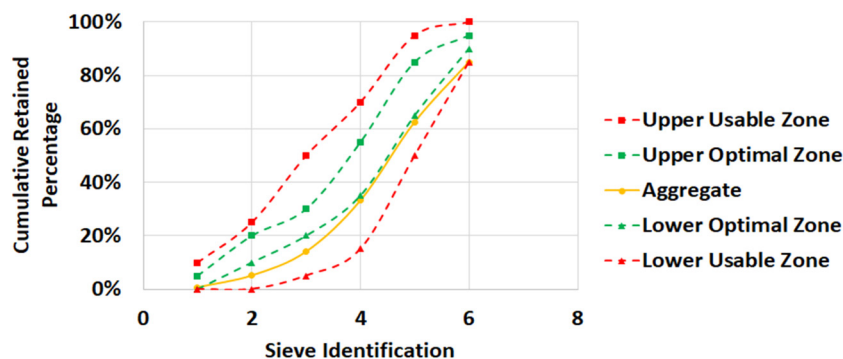


Figure S2 – Sand granulometric curve
Source: Authors

For this research, graphene oxide (GO) nanoparticles were synthesized using a modified Hummers method, as illustrated in Figs. S3(a)–S3(f) [1]. During the synthesis process, 1 g of graphite was dispersed in a jar with NaNO_3 and H_2SO_4 under continuous agitation for one hour. Then, 3 g of KMnO_4 were gradually added (1 g every 15 minutes) while maintaining an ice bath to keep the solution temperature below 20°C , preventing overheating and potential hazards. The mixture was then vigorously stirred before slowly adding 100 ml of heated distilled water for dilution. Subsequently, 3 ml of a 30% H_2O_2 solution were added to ensure the complete reaction of KMnO_4 , followed by a resting period. Finally, the mixture was washed with HCl and water, filtered, and dried to obtain the final GO product.

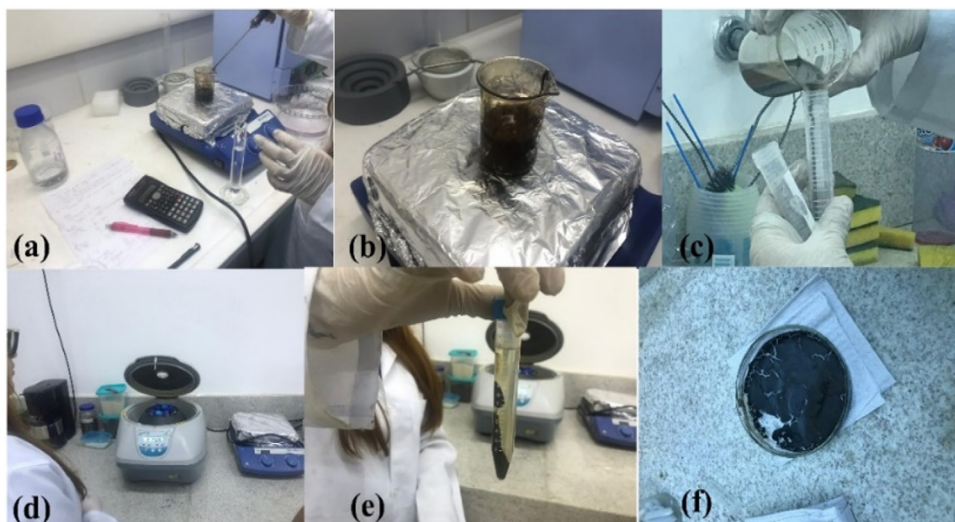


Figure S3 – GO nanoparticles obtained through the modified method of Hummers.

Source: Authors

The addition of 0.1872 g of GO to the mortar was carried out through manual pre-dilution, followed by uniform agitation for 1 minute using a magnetic stirrer before application. The execution of this process is shown in Fig. S4.



Figure S4 – Nanoparticles of GO dispersion

Source: Authors

To prepare the test specimens, reference samples and samples with 0.03% graphene oxide (GO) were produced. The mix ratio was 1:3:0.48 (cement:sand:water), with 624 g of cement, 1872 g of sand, and 300 ml of water, maintaining a water/cement ratio of 0.48. The GO nanoparticles (0.1872 g per specimen) were pre-dispersed in part of the mixing water before incorporation. Specimens were molded following [2] and mixed using a mechanical mixer.

The mortar molds were prepared in four layers of approximately equal height, with each layer compacted manually using a tamper with 30 blows after applying a release agent to the molds. Following molding, the test specimens remained in the molds for 24 hours. A total of 12 cylindrical specimens (5 × 10 cm) was produced, including six with GO and six without, as shown in Flg. S5.



Figure S5 – (a) Test specimens with GO addition, after demolding; and (b) Test specimens without GO addition, after demolding.

References

- [1] A. Alazmi, S. Rasul, S.P. Patole, P.M.F.J. Costa, "Comparative study of synthesis and reduction methods for graphene oxide," *Polyhedron*, vol. 116, pp. 153-161, Sep. 2016. <https://doi.org/10.1016/j.poly.2016.04.044>.
- [2] NBR 7215, /*Portland cement – Determination of compressive strength of cylindrical test specimens*/, NBR 7215, Brazilian Association of Technical Standards. Rio de Janeiro, Brazil, 2019.